

Article

Antiseizure Properties of Histamine H₃ Receptor Antagonists Belonging 3,4-Dihydroquinolin-2(1H)-Ones

Yi Hua ^{1,†}, Mingxia Song ^{1,†}, Qiaoyue Guo ¹, Yiqin Luo ¹, Xianqing Deng ^{1,*} and Yushan Huang ^{2,*}¹ Health Science Center, Jinggangshan University, Ji'an 343009, China² Center for Evidence Based Medical and Clinical Research, First Affiliated Hospital of Gannan Medical University, Ganzhou 341000, China

* Correspondence: xqdeng@jgsu.edu.cn (X.D.); huangyushan@gmu.edu.cn (Y.H.)

† These authors contributed equally to this work.

Abstract: H₃R is becoming an attractive and promising target for epilepsy treatment as well as the discovery of antiepileptics. In this work, a series of 6-aminoalkoxy-3,4-dihydroquinolin-2(1H)-ones was prepared to screen their H₃R antagonistic activities and antiseizure effects. The majority of the target compounds displayed a potent H₃R antagonistic activity. Among them, compounds **2a**, **2c**, **2h**, and **4a** showed submicromolar H₃R antagonistic activity with an IC₅₀ of 0.52, 0.47, 0.12, and 0.37 μM, respectively. The maximal electroshock seizure (MES) model screened out three compounds (**2h**, **4a**, and **4b**) with antiseizure activity. Meanwhile, the pentylenetetrazole (PTZ)-induced seizure test gave a result that no compound can resist the seizures induced by PTZ. Additionally, the anti-MES action of compound **4a** fully vanished when it was administrated combined with an H₃R agonist (RAMH). These results showed that the antiseizure role of compound **4a** might be achieved by antagonizing the H₃R receptor. The molecular docking of **2h**, **4a**, and PIT with the H₃R protein predicted their possible binding patterns and gave a presentation that **2h**, **4a**, and PIT had a similar binding model with H₃R.

Keywords: antiepileptics; antiseizure; anticonvulsant; H₃R antagonists; 3,4-dihydroquinolin-2(1H)-one

Citation: Hua, Y.; Song, M.; Guo, Q.; Luo, Y.; Deng, X.; Huang, Y. Antiseizure Properties of Histamine H₃ Receptor Antagonists Belonging 3,4-Dihydroquinolin-2(1H)-Ones. *Molecules* **2023**, *28*, 3408. <https://doi.org/10.3390/molecules28083408>

Academic Editors:
Diego Muñoz-Torrero and
Cristobal De Los Rios

Received: 19 March 2023
Revised: 10 April 2023
Accepted: 10 April 2023
Published: 12 April 2023



Copyright: © 2023 by the authors. Licensee MDPI, Basel, Switzerland. This article is an open access article distributed under the terms and conditions of the Creative Commons Attribution (CC BY) license (<https://creativecommons.org/licenses/by/4.0/>).

1. Introduction

Histamine, an endogenous biological amine, mediates various physiological and pathological processes by acting on four histamine receptors in the G protein-coupled receptor (GPCR) family [1]. Among them, histamine H₁ receptors (H₁R) and histamine H₂ receptors (H₂R) are related to anaphylactic reaction and the secretion of gastric acid, respectively. Histamine H₄ receptors (H₄R) are mainly involved in the human body's immune response. Histamine H₃ receptors (H₃R) are mainly expressed in the central nervous system (CNS). As one of the auto-receptors, it negatively regulates the synthesis and secretion of histamine in the CNS [2]. Recently it was reported as relating to the physiological processes of sleep, awakening, appetite, and learning and memory [3,4]. H₃R has become a potentially important target for the diseases of narcolepsy, Alzheimer's, schizophrenia, learning and memory disorders, and epilepsy [5,6].

In particular, as an inhibitory heteroreceptor, H₃R can affect the level of some neurotransmitters, such as serotonin, norepinephrine, γ-aminobutyric acid, and glutamate in the CNS related to epilepsy [7–9]. It has been proved that H₃R antagonists can treat epilepsy by promoting the synthesis and secretion of histamine [10–12]. In addition, some studies have reported that H₃R antagonists have obvious protective effects on NMDA-induced neuronal damage and cell death [13–15]. Therefore, increasing attention has been focused on H₃R in epilepsy treatment.

In the last two decades, increasing antagonists or inverse agonists of H₃R have been prepared and identified with antiseizure activity in several kinds of epileptic animal models [16–18]. Pitolisant (PIT), an H₃R antagonist and inverse agonist, was approved in

the EU for narcolepsy treatment. Meanwhile, it also has been subjected to clinical Phase II trials to treat photosensitive epilepsy [19]. The results showed that PIT can inhibit photosensitive epilepsy and gave a profitable electroencephalogram (EEG) performance when taken at the dose of 30 mg or 60 mg [20]. In addition, PIT displayed a powerful antiseizure activity in the electrical kindling model of epilepsy [21].

In our previous work, dozens of 2-methyl-4-phenyloxazoles were designed and synthesized as new H₃R antagonists [22]. All these compounds showed micromolar to submicromolar H₃R antagonistic activities. In addition, some of them displayed an antiseizure activity in the maximal electroshock seizure (MES) test. It is interesting to note that the antiseizure activity of the representative compound I (Figure 1, I) completely vanished when it was administrated combined with an H₃R agonist R-(α)-methylhistamine (RAMH), which confirmed the correlation between H₃R inhibition and antiepileptic activity.

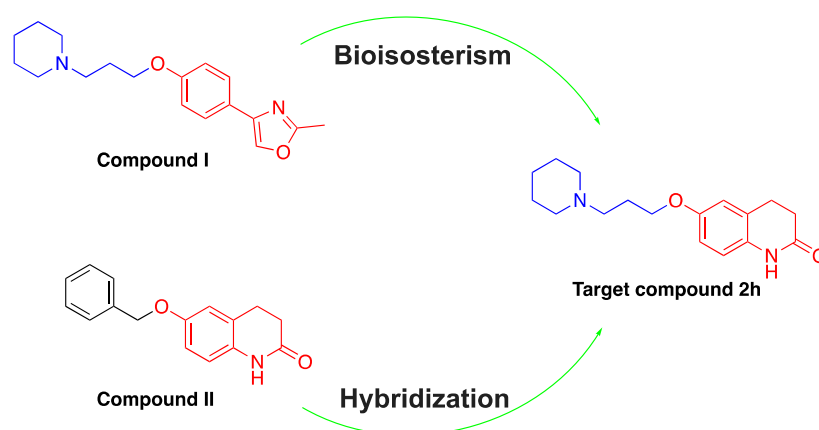


Figure 1. The structures of reported anticonvulsive compounds I, II, and target compound 2h.

To continue the program of developing antiseizure drugs from an H₃R antagonist, herein, the 2-methyl-4-phenyloxazole moiety of the compound I was interchanged by 3,4-dihydroquinolin-2(1H)-one to obtain a potential H₃R antagonist (Figure 1, compound 2h). The 3,4-dihydroquinolin-2(1H)-one is an eminent pharmaceutical skeleton, which has been utilized to obtain great amounts of compounds with an antiseizure activity [23–25]. The hybridization of compounds I and II is expected to obtain new H₃R antagonists with better antiseizure activity. Apart from compound 2h, analogs (2a–2g, 2i) using various kinds of amines replacing the piperidine group in compound 2h, and derivatives (3a–3c, 4a–4b) via adjusting the length of the link and introducing the substituents at the N atom of amide, were also synthesized.

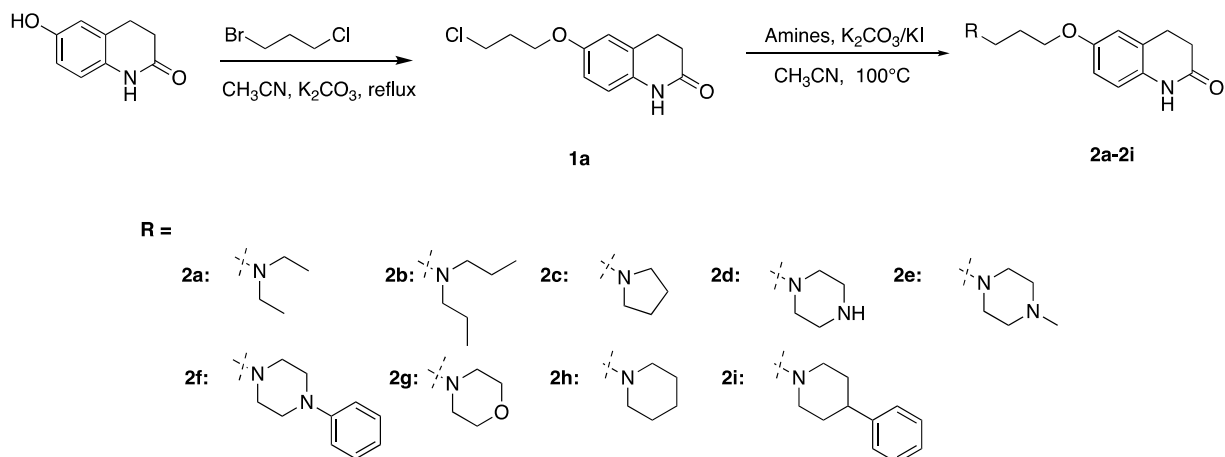
All the titled compounds were synthesized smoothly and structurally confirmed by ¹NMR, ¹³NMR, and HR-MS. Luciferase assay based on the cAMP-response element (CRE) was used to screen the H₃R antagonism activity. Two widely used epileptic animal models, the MES model and pentylenetetrazole (PTZ)-induced seizure model, were applied to evaluate the antiseizure activity. In addition, molecular docking was carried out to understand the molecular basis of the H₃R antagonistic activity of the prepared compounds. We hope that through this study, a new H₃R antagonistic skeleton can be investigated to accelerate the discovery of new antiseizure drugs.

2. Results and Discussion

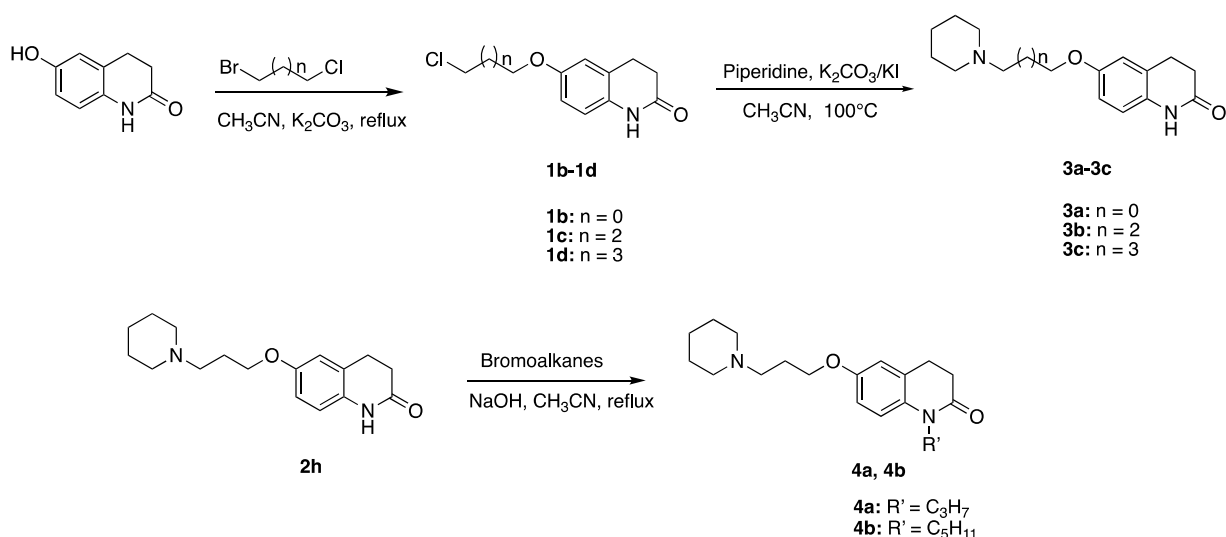
2.1. Chemistry

The synthetic route of compounds 2a–2i through a two-step route is shown in Scheme 1. Compounds 3a–3c and 4a–4b were prepared smoothly as shown in Scheme 2. Briefly, compounds 1a–1d were synthesized by the reaction of 6-hydroxyquinolinone with dihaloalkane in the presence of K₂CO₃. The substitution reaction of compound 1a with appropriate secondary amines gave compounds 2a–2i. The substitution reaction of compounds 1b–1d

with piperidine provided compound **3a-3c**. Finally, compounds **4a** and **4b** were achieved by an alkylation of compound **2h**.



Scheme 1. The synthesis of a first series of 3,4-dihydroquinolin-2(1H)-ones **2a-2i**.



Scheme 2. The synthesis of a second and third series of 3,4-dihydroquinolin-2(1H)-ones **3a-3c** and **4a-4b**.

2.2. Pharmacology

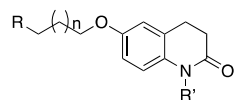
2.2.1. Screen for H₃R Antagonistic Activity

CRE luciferase reporter assays are widely applied for the high-throughput screening of GPCR agonists and antagonists [26,27], which was used to screen the H₃R antagonistic activities of the titled compounds (**2a-2i**, **3a-3c**, and **4a-4b**) in this work. PIT was used as a positive drug.

The results of targets **2a-2i**, **3a-3c**, and **4a-4b** as H₃R antagonists are summarized in Table 1. The majority of the synthesized compounds displayed outstanding H₃R antagonistic activities. Among them, compounds **2a** ($IC_{50} = 0.52 \mu M$), **2c** ($IC_{50} = 0.47 \mu M$), **2h** ($IC_{50} = 0.12 \mu M$), and **4a** ($IC_{50} = 0.37 \mu M$) displayed antagonistic activities at a submicromolar level. PIT showed H₃R antagonistic activity with IC_{50} of $0.69 \mu M$ at the same condition. When the diethyl in compound **2a** was replaced by dipropyl, the H₃R antagonistic activity decreased significantly with the IC_{50} of compound **2b** higher than $50 \mu M$. When a phenyl group was introduced onto the piperidine of compound **2h**, the H₃R antagonistic activity of compound **2i** declined dozens of times. This suggested that substituted tertiary amine with appropriate volume is required for the H₃R antagonistic activity. Altering the link length

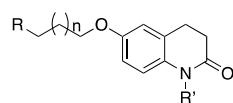
of compound **2h** to obtain compounds **3a**, **3b**, and **3c**. It can be seen that the best chain length of the carbons is three, which gave the compound **2h** an IC_{50} of 0.12 μ M. The H_3R antagonistic activity decreased when the chain length became longer or shorter. Among the cyclic amine compounds, the pyrrole and piperidine substituted compounds (**2c** and **2h**) showed higher antagonistic activities than the compounds coupled with piperazine and morpholine (**2d–2g**). This may be the result of the lipophilic binding of the tertiary amine with the receptor [28]

Table 1. H_3R antagonistic effects of targets **2a–2i**, **3a–3c**, and **4a–4b**.



| Compounds | R | n | R' | H_3R Antagonistic Activity (IC_{50} , μ M) | ClogP ^a |
|-----------|---|---|----|---|--------------------|
| 2a | | 1 | H | 0.52 | 2.72 |
| 2b | | 1 | H | >50 | 3.78 |
| 2c | | 1 | H | 0.47 | 2.29 |
| 2d | | 1 | H | >50 | 1.23 |
| 2e | | 1 | H | 38.11 | 0.74 |
| 2f | | 1 | H | 25.64 | 3.63 |
| 2g | | 1 | H | 46.04 | 1.64 |
| 2h | | 1 | H | 0.12 | 2.85 |
| 2i | | 1 | H | 38.47 | 4.26 |
| 3a | | 0 | H | 7.49 | 2.55 |

Table 1. Cont.



| Compounds | R | n | R' | H ₃ R Antagonistic Activity (IC ₅₀ , μM) | ClogP ^a |
|-----------|---|---|--------------------------------|--|--------------------|
| 3b | | 2 | H | 2.88 | 2.96 |
| 3c | | 3 | H | >50 | 3.49 |
| 4a | | 1 | C ₃ H ₇ | 0.37 | 3.98 |
| 4b | | 1 | C ₅ H ₁₁ | 1.91 | 5.03 |
| PIT | - | - | - | 0.69 | 4.82 |

^a ClogP was calculated by ChemDraw 16.0 (CambridgeSoft, Cambridge, MA, USA).

2.2.2. Evaluation of the Antiseizure Activity

To find new antiseizure candidates, the antiseizure activities of the titled compounds were evaluated via two seizure models in mice, while using PIT and antiepileptic valproic sodium (VPA) as positive controls. One of the two test models is the MES seizure model, another is the PTZ-induced seizure model. In our previous work, we found that the synthetic H₃R antagonists and PIT showed an antiseizure activity at 10 mg/kg [22]. In addition, the administration of this dosage can minimize the impact of other possible side effects such as central inhibition and cardiac toxicity. The dose of the H₃R antagonists **2a-2i**, **3a-3c**, **4a-4b**, and PIT was chosen as 10 mg/kg. In addition, the tested dose of VPA was 300 mg/kg.

It could be seen that all animals in the control group experienced hindlimb stiffness after the electrical stimulation in the MES model. In the treated group, the definition of protection was the reduction or vanishing of the tonic hind limb extension (THLE) in mice. As shown in Figure 2, compounds **2h**, **4a**, and **4b** as well as PIT and VPA decreased the duration of THLE significantly ($p < 0.05$, or $p < 0.001$), and showed good protection for mice. The majority of the compounds showing H₃R antagonistic activity in Table 1 did not exhibit antiseizure activity in the MES model. However, compounds **2a**, **2c**, and **2h** hold higher H₃R antagonistic activity and displayed a descending effect for the duration of THLE, although the effect of compounds **2a** and **2c** has no significant difference. Compounds **4a** and **4b** showed an antiseizure activity in the MES with a significant decrease in the THLE in mice. The two compounds were substituted by an alkyl group on the quinolinone, which increased their ClogP value (as seen in Table 1). This may be an important contributor to their in vivo antiseizure activity in the MES test, because marketed antiepileptics usually have a high ClogP to assure their penetration through the blood–brain barrier and run up to the site of action.

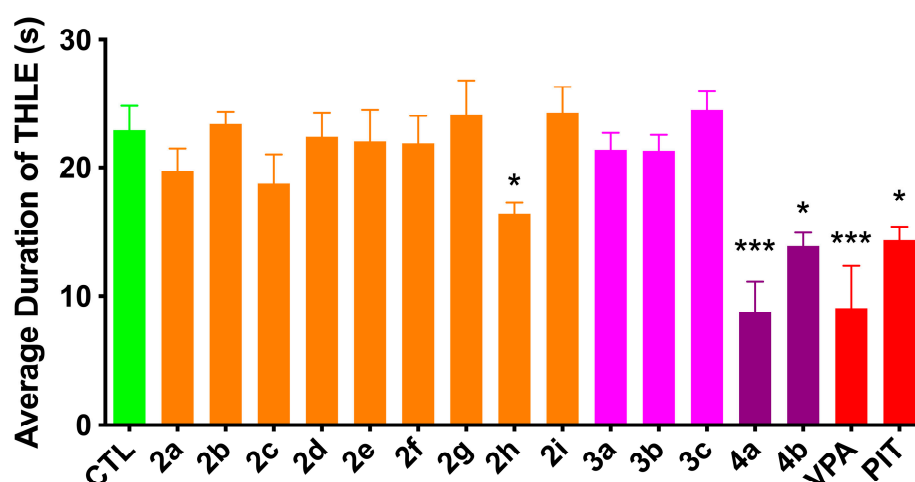


Figure 2. The protection of H₃R antagonists **2a-2i**, **3a-3c**, **4a-4b** (10 mg/kg, i.p.), PIT (10 mg/kg, i.p.), and the antiepileptic drug VPA (300 mg/kg, i.p.) in the maximal electroshock seizure model. The definition of protection was the reduction or vanishing of the tonic hind limb extension (THLE). Data are shown as mean \pm SEM in the figure, which are derived from seven animals in each group. * $p < 0.05$, *** $p < 0.001$ when compared to the control group (CTL).

The PTZ model was usually used to screen the antiepileptic candidates for the absence of seizures. In this work, compounds **2a-2i**, **3a-3c**, and **4a-4b** were also evaluated for their antiseizure action in the PTZ model in mice, while using VPA as the positive drug. As shown in Figure 3, no compound relieved the seizures induced by PTZ at the dose of 10 mg/kg (i.p.). PIT also did not exhibit protection in mice at the same dose. While VPA fully inhibited the seizure induced by PTZ when pretreated with the dosage of 300 mg/kg. The failure of synthesized compounds in the PTZ model is expected because our previously reported H₃R inhibitors were also ineffective in the PTZ model [22]. The failure of the PIT in the PTZ model also occurred in Sadek's study [29]. These contradictory effects observed for the synthesized H₃R inhibitors and PIT in the MES and PTZ models might relate to the different levels of histamine release resulting from the seizures in different seizure models [17]. A considerable increase in histamine levels was found in the brain after MES-induced seizures, whereas a tendency toward a decrease in histamine levels was observed after PTZ-kindled convulsions [30].

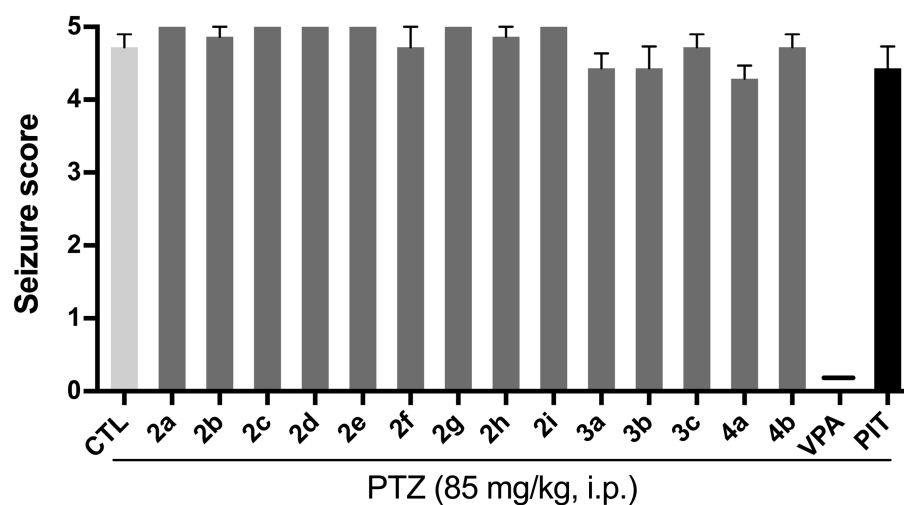


Figure 3. The performance of compounds **2a-2i**, **3a-3c**, and **4a-4b** (10 mg/kg, i.p.), H₃R antagonist PIT (10 mg/kg, i.p.), and antiepileptic VPA (300 mg/kg, i.p.) in the PTZ-induced seizure model. The seizure scores came from seven animals in each group and are shown as mean \pm SEM in the figure. This represents that VPA fully inhibited the convulsive behavior induced by PTZ.

Based on the better performance of compounds **2h**, **4a**, and **4b** in the MES seizure model, they were selected for further studies. To obtain the accurate effective dose of compounds **2h**, **4a**, and **4b** in the MES model, different dosages of three compounds were applied in the MES test. Inspiringly, the protective effect was obtained in a dose-dependent manner, although the effects at the lowest dosage (3 mg/kg) have no significant difference. As shown in Figure 4, the H₃R antagonist PIT also exhibited a dose-dependent antiseizure activity. In particular, PIT fully abolished the THLE induced by MES at 30 mg/kg, confirming its potential antiseizure activity.

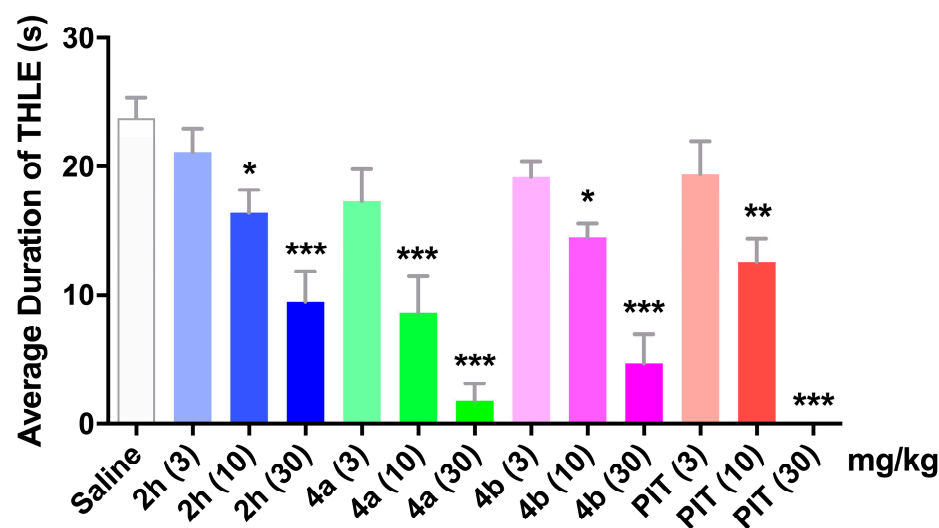


Figure 4. The protection of compounds **2h**, **4a**, **4b**, and PIT against the maximal electroshock-induced seizures in doses of 3, 10, and 30 mg/kg. * $p < 0.05$, ** $p < 0.01$, *** $p < 0.001$ when compared to the control group (saline).

A rotarod test was carried out to estimate the neurological safety of compounds **2h**, **4a**, and **4b**. As described in Table 2, no compound showed neurotoxicity at the dose of 10 mg/kg and 30 mg/kg. Compound **2h** showed neurotoxicity with one mouse in three at 100 mg/kg, while compounds **4a**, **4b** and PIT showed no neurotoxicity at 100 mg/kg. At the dose of 300 mg/kg, all animals treated with compound **2h** and two-thirds of mice treated with compounds **4a** and **4b** were dead, which indicated that these compounds showed toxicity at the higher dose.

Table 2. The neurotoxicity of compounds **2h**, **4a**, and **4b** (i.p.) in the rotarod test in mice.

| Compounds | Neurotoxicity | | |
|-----------|---------------|----------|-----------|
| | 10 mg/kg | 30 mg/kg | 100 mg/kg |
| 2h | 0/3 | 0/3 | 1/3 |
| 4a | 0/3 | 0/3 | 0/3 |
| 4b | 0/3 | 0/3 | 0/3 |
| PIT | 0/3 | 0/3 | 0/3 |

Up to now, we have screened out some antiepileptic compounds from the H₃R antagonists belonging to 3,4-dihydroquinolin-2(1*H*)-ones, especially from the molecules with a strong H₃R inhibitory activity. However, whether their antiepileptic activity comes from their antihistamine activity is unknown. To make this clear, the ability of compound **4a** to decrease the duration of THLE in the MES model was re-evaluated in the mice pretreated by RAMH (10 mg/kg, i.p.). RAMH, as a CNS-penetrant histamine H₃R agonist, can vanish or weaken the antihistamine effects of histamine antagonists. As shown in Figure 5, when co-injected with RAMH, compound **4a** cannot decrease the duration of THLE ($p > 0.05$).

This result confirmed that the H₃R antagonism of **4a** was an important mechanism for its antiseizure activity.

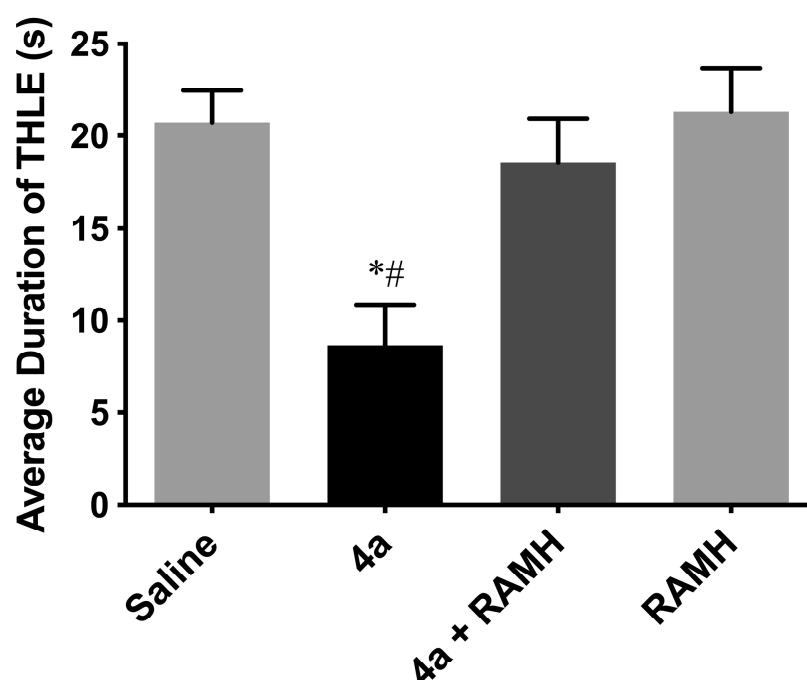


Figure 5. The protection of compound **4a** (10 mg/kg, i.p.) against the maximal electroshock-induced seizures in mice pretreated with RAMH (10 mg/kg, i.p.). Data come from seven animals in each group and are shown as mean \pm SEM in the figure. * $p < 0.01$ when compared to the control group (saline-treated), # $p < 0.01$ when compared to the combined group (**4a** + RAMH).

2.3. Molecular Docking

To make clear the molecular binding mode of the titled compounds with H₃R and understand the molecular basis of their H₃R antagonistic activity, the molecular docking of **2h**, **4a**, and PIT with the H₃R protein was carried out. In this docking study, the 3D structure of H₃R was constructed from the structure-known H₁R protein (PDB ID: 3RZE) by homology modeling [31].

As shown in Figure 6, compounds **2h**, **4a**, and PIT bound to H₃R in the same binding pocket and had similar binding patterns. The piperidine group in the compounds **2h** and **4a** formed a Pi–Pi interaction with the amino acid residue Pro184 of H₃R. The phenyl group on the quinoline ring bound to the amino acid residues Tyr115 and Met378 with Pi–Pi force and alkyl interaction, respectively. The amide group in compound **2h** formed a critical H-bond interaction with Glu206 and Ser203, while this interaction vanished in the docking of compound **4a** because of the hinder of the N-substitution. This may be the important reason for the lower H₃R antagonistic activity of **4a** than **2h**. However, the propyl group in compound **4a** formed hydrophobic interactions with Tyr374 and Met378. PIT and H₃R interacted through the similar amino acid residues Tyr115, Pro184, His187, Ala190, Ala202, Glu206, Trp371, Met378, and so on. The overlying pattern of compounds **2h**, **4a**, and PIT was shown in Figure 7, which vividly presented that **2h**, **4a**, and PIT had a similar binding model with H₃R. The docking score for compound **2h** and H₃R protein binding pocket was obtained to be 115.14, which is higher than that of compound **4a** and PIT with a score of 109 and 103.19, respectively. The docking score is consistent with their antihistamine effects. These results supported the suggestion that compounds **2h** and **4a** play their antiseizure effects by binding and inhibiting the H₃R receptor, with a similar binding model to PIT.

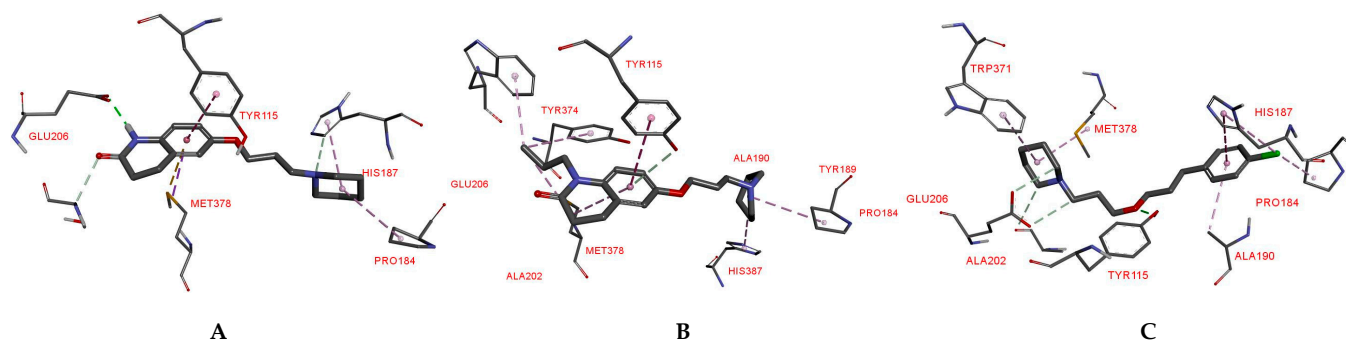


Figure 6. The predicted binding configurations when **2h** (A), **4a** (B), and PIT (C) dock with H₃R.

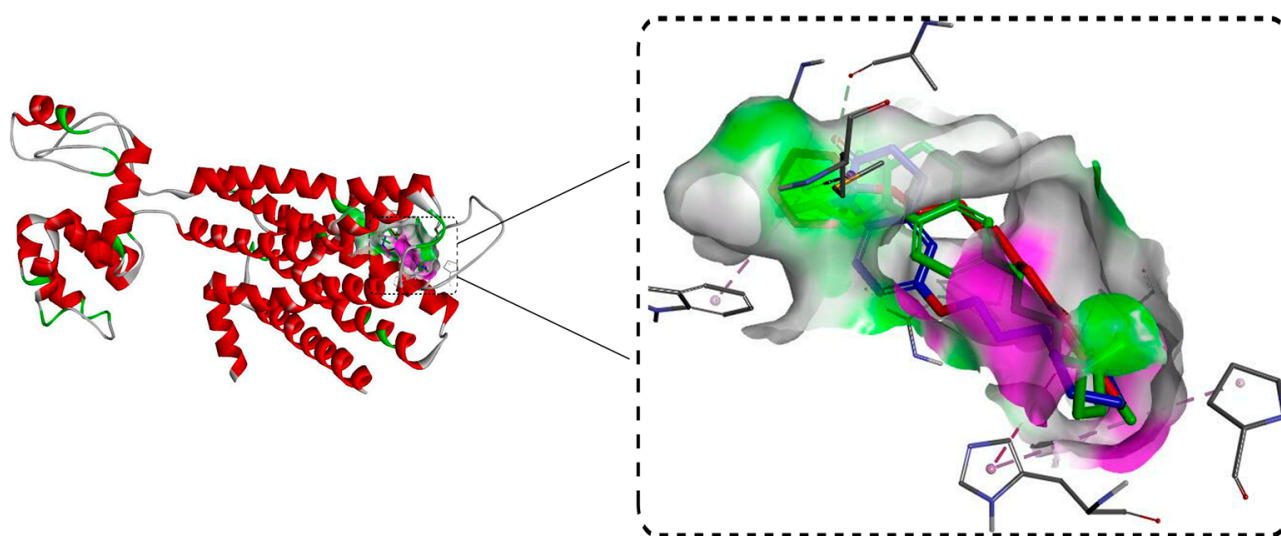


Figure 7. The overlying pattern of compound **2h** (blue), **4a** (green), and PIT (red) in the binding pocket of the H₃R.

3. Materials and Methods

3.1. Chemical Part

Unless otherwise specified, the reagents used in this work were bought from Macklin Inc. All the reactions were monitored by thin-layer chromatography (TLC). After purification, the products were sent to the analysis center for a structure confirmation. The NMR spectrums were measured on a Bruker AV-300 spectrometer. The HR-MS of compounds was measured on a Xevo G2-XS QTOF mass spectrometer.

3.1.1. Synthesis Procedure of 6-(Chloroalkoxy)-3,4-dihydroquinolin-2(1H)-one (**1a-1d**)

Taking compound **1a** as an example: 6-hydroxyquinolinone (1.63 g, 10 mmol), 1-bromo-3-chloropropane (1.87 g, 12 mmol), and potassium carbonate (2.76 g, 20 mmol) were added into a round-bottomed flask with 20 mL acetonitrile. After refluxing the mixture for 24 h, the finish of the reaction was identified by the TLC monitoring with 25% ethyl acetate in petroleum ether. Then the solvent was removed and the leavings were purified using silica gel column chromatography (1% methanol in DCM) to obtain the compound **1a**. The compounds **1b-1d** were obtained according to the above method using the other haloalkanes. The characterization for the four compounds is listed below.

6-(3-Chloropropoxy)-3,4-dihydroquinolin-2(1H)-one (**1a**) Mp 99–102 °C, yield 79%. ¹H-NMR (CDCl₃, 300 MHz): δ 2.20–2.27 (m, 2H, OCH₂CH₂), 2.63 (t, 2H, J = 8.5 Hz, CH₂), 2.95 (t, 2H, J = 8.5 Hz, CH₂), 3.75 (t, 2H, J = 6.3 Hz, ClCH₂), 4.09 (t, 2H, J = 6.3 Hz, OCH₂), 6.72–6.81 (m, 3H, Ph-H), 9.32 (s, 1H, CONH). ¹³C-NMR (DMSO-*d*₆, 75 MHz): δ 171.9, 154.7, 131.1, 125.0, 116.4, 114.5, 113.2, 64.7, 41.5, 32.3, 30.6, 25.7. HR-MS (ESI) calcd for C₁₂H₁₅ClNO₂⁺ ([M + H]⁺): 240.0786; found: 240.0791.

6-(2-Chloroethoxy)-3,4-dihydroquinolin-2(1H)-one (**1b**) Mp 151–152 °C, yield 81%. ¹H-NMR (CDCl₃, 300 MHz): δ 2.63 (t, 2H, *J* = 8.6 Hz, CH₂), 2.96 (t, 2H, *J* = 8.5 Hz, CH₂), 3.81 (t, 2H, *J* = 5.8 Hz, ClCH₂), 4.21 (t, 2H, *J* = 5.8 Hz, OCH₂), 6.76–6.78 (m, 3H, Ph-H), 8.76 (s, 1H, CONH). ¹³C-NMR (DMSO-*d*₆, 75 MHz): δ 171.5, 154.1, 131.5, 125.2, 116.2, 115.0, 113.5, 68.6, 41.9, 30.6, 25.7. HR-MS (ESI) calcd for C₁₁H₁₃ClNO₂⁺ ([M + H]⁺): 226.0629; found: 226.0628.

6-(4-Chlorobutoxy)-3,4-dihydroquinolin-2(1H)-one (**1c**) Mp 146–148 °C, yield 71%. ¹H-NMR (CDCl₃, 300 MHz): δ 1.91–1.99 (m, 4H, OCH₂(CH₂)₂), 2.61 (t, 2H, *J* = 7.6 Hz, CH₂), 2.93 (t, 2H, *J* = 7.7 Hz, CH₂), 3.62 (t, 6H, *J* = 5.8 Hz, N-CH₂), 3.96 (t, 2H, *J* = 6.2 Hz, O-CH₂), 6.69–6.75 (m, 3H, Ph-H), 8.85 (s, 1H, CONH). ¹³C-NMR (CDCl₃, 75 MHz): δ 171.6, 154.9, 130.9, 125.0, 116.3, 114.5, 113.1, 67.4, 44.7, 30.6, 29.3, 26.7, 25.7. HR-MS (ESI) calcd for C₁₃H₁₇ClNO₂⁺ ([M + H]⁺): 254.0942; found: 254.0947.

6-((5-Chloropentyl)oxy)-3,4-dihydroquinolin-2(1H)-one (**1d**) Mp 128–130 °C, yield 72%. ¹H-NMR (CDCl₃, 300 MHz): δ 1.59–1.93 (m, 6H, OCH₂(CH₂)₃), 2.62 (t, 2H, *J* = 7.6 Hz, COCH₂), 2.93 (t, 2H, *J* = 7.6 Hz, PhCH₂), 3.56 (t, 2H, *J* = 5.9 Hz, ClCH₂), 3.93 (t, 2H, *J* = 6.2 Hz, OCH₂), 6.69–6.81 (m, 3H, Ph-H), 9.51 (s, 1H, CONH). ¹³C-NMR (DMSO-*d*₆, 75 MHz): δ 172.0, 154.9, 130.9, 124.9, 116.4, 114.4, 113.1, 68.0, 44.9, 32.3, 30.6, 28.6, 25.7, 23.5. HR-MS (ESI) calcd for C₁₄H₁₉ClNO₂⁺ ([M + H]⁺): 268.1099; found: 268.1106.

3.1.2. The Synthesis Procedure of

6-(3-Substituted-aminopropoxy)-3,4-dihydroquinolin-2(1H)-one (**2a-2i**) and Its Analogues (**3a-3c**)

Taking compound **2a** as an example: compounds **1a** (1.20 g, 5 mmol), diethylamine (0.73 g, 10 mmol), K₂CO₃ (1.38 g, 10 mmol), and KI (1.0 g, 6 mmol) were added to a round-bottomed flask with 20 mL acetonitrile. After refluxing the mixture for 24 h, the finish of the reaction was confirmed by the TLC monitoring with 50% ethyl acetate in a petroleum ether. After cooling to room temperature, the mixture was filtered, and the filtrate was evaporated to obtain a crude product, which was purified on silica gel column chromatography (1.5% MeOH in DCM) to obtain compound **2a**. Compounds **2b-2i** were prepared according to the above method with the compound **1a** and other secondary amines. The compounds **3a** (**3b**, **3c**) were prepared according to the above method with the compounds **1b** (**1c**, **1d**) and piperidine. The characterization for these compounds is listed below.

6-(3-(Diethylamino)propoxy)-3,4-dihydroquinolin-2(1H)-one hydrochloride (**2a**) Mp 68–70 °C, yield 76%. ¹H-NMR (DMSO-*d*₆, 300 MHz): δ 1.23 (t, 6H, *J* = 7.6 Hz, CH₃), 2.08–2.15 (m, 2H, CH₂), 2.38 (t, 2H, *J* = 7.5 Hz, CH₂), 2.82 (t, 2H, *J* = 7.5 Hz, CH₂), 3.05–3.17 (m, 6H, N-CH₂), 4.00 (t, 2H, *J* = 6.0 Hz, O-CH₂), 6.72–6.81 (m, 3H, Ph-H), 9.93 (s, 1H, CONH), 10.81 (s, 1H, HCl). ¹³C-NMR (DMSO-*d*₆, 75 MHz): δ 170.21, 153.36, 132.46, 125.34, 116.25, 114.65, 113.53, 65.64, 46.57, 43.13, 30.79, 25.53, 23.54, 8.87. HR-MS (ESI) calcd for C₁₆H₂₅N₂O₂⁺ ([M + H]⁺): 277.1911; found: 277.1912.

6-(3-(Dipropylamino)propoxy)-3,4-dihydroquinolin-2(1H)-one hydrochloride (**2b**) Mp 57–59 °C, yield 71%. ¹H-NMR (DMSO-*d*₆, 300 MHz): δ 0.96 (t, 6H, *J* = 7.5 Hz, CH₃), 1.71–1.84 (m, 4H, CH₂), 2.17–2.22 (m, 2H, CH₂), 2.43 (t, 2H, *J* = 7.5 Hz, CH₂), 2.84 (t, 2H, *J* = 7.5 Hz, CH₂), 2.98–3.05 (m, 4H, N-CH₂), 3.20–3.26 (m, 2H, N-CH₂), 3.99 (t, 2H, *J* = 5.6 Hz, O-CH₂), 6.61–6.79 (m, 3H, Ph-H), 9.84 (s, 1H, CONH), 10.73 (s, 1H, HCl). ¹³C-NMR (DMSO-*d*₆, 75 MHz): δ 175.10, 158.50, 137.05, 129.70, 121.09, 119.07, 118.00, 70.02, 59.02, 54.72, 35.56, 30.48, 28.39, 21.78, 16.03. HR-MS (ESI) calcd for C₁₈H₂₉N₂O₂⁺ ([M + H]⁺): 305.2224; found: 305.2223.

6-(3-(Pyrrolidin-1-yl)propoxy)-3,4-dihydroquinolin-2(1H)-one hydrochloride (**2c**) Mp 120–122 °C, yield 83%. ¹H-NMR (DMSO-*d*₆, 300 MHz): δ 1.86–2.07 (m, 6H, CH₂), 2.40 (t, 2H, *J* = 7.5 Hz, CH₂), 2.84 (t, 2H, *J* = 7.5 Hz, CH₂), 3.05 (s, 2H, N-CH₂), 3.33 (s, 2H, N-CH₂), 3.59 (s, 2H, N-CH₂), 4.00 (s, 2H, *J* = 6.0 Hz, O-CH₂), 6.3–6.80 (m, 3H, Ph-H), 9.44 (s, 1H, CONH), 9.90 (s, 1H, HCl). ¹³C-NMR (DMSO-*d*₆, 75 MHz): δ 170.22, 153.79, 132.50, 125.34, 116.24, 114.60, 113.59, 65.41, 53.89, 51.94, 30.80, 25.89, 25.55, 23.06. HR-MS (ESI) calcd for C₁₆H₂₃N₂O₂⁺ ([M + H]⁺): 275.1754; found: 275.1755.

6-(3-(Piperazin-1-yl)propoxy)-3,4-dihydroquinolin-2(1H)-one (**2d**) Mp 150–151 °C, yield 78%. ¹H-NMR (DMSO-*d*₆, 300 MHz): δ 1.77–1.86 (m, 2H, CH₂), 2.37–2.51 (m, 12H, CH₂), 2.83 (t, 2H, *J* = 7.2 Hz, N-CH₂), 3.92 (t, 2H, *J* = 6.1 Hz, O-CH₂), 6.69–6.76 (m, 3H, Ph-H), 9.86 (s, 1H, N-H). ¹³C-NMR (DMSO-*d*₆, 75 MHz): δ 170.19, 154.28, 132.15, 125.28, 116.23, 114.48, 113.45, 66.53, 55.15, 53.11, 46.11, 30.84, 26.76, 25.57, HR-MS (ESI) calcd for C₁₆H₂₄N₃O₂⁺ ([M + H]⁺): 290.1863; found: 290.1864.

6-(3-(4-Methylpiperazin-1-yl)propoxy)-3,4-dihydroquinolin-2(1H)-one (**2e**) Mp 159–160 °C, yield 79%. ¹H-NMR (DMSO-*d*₆, 300 MHz): δ 1.49–1.67 (m, 7H, CH₂, NCH₃), 1.95–2.05 (m, 2H, CH₂), 2.40 (t, 2H, *J* = 7.6 Hz, N-CH₂), 2.81–2.89 (m, 8H, N-CH₂), 3.97 (t, 2H, *J* = 6.2 Hz, O-CH₂), 6.70–6.79 (m, 3H, Ph-H), 9.89 (s, 1H, CONH). ¹³C-NMR (DMSO-*d*₆, 75 MHz): δ 170.19, 153.98, 132.39, 125.32, 116.24, 114.57, 113.56, 65.98, 54.54, 53.35, 30.82, 25.56, 25.01, 24.13, 22.75. HR-MS (ESI) calcd for C₁₇H₂₆N₃O₂⁺ ([M + H]⁺): 304.2020; found: 304.2015.

6-(3-(4-Phenylpiperazin-1-yl)propoxy)-3,4-dihydroquinolin-2(1H)-one (**2f**) Mp 199–201 °C, yield 80%. ¹H-NMR (DMSO-*d*₆, 300 MHz): δ 1.89 (t, 2H, *J* = 6.2 Hz, CH₂), 2.37–2.51 (m, 8H, CH₂), 2.83 (t, 2H, *J* = 7.3 Hz, CH₂), 3.12 (s, 4H, CH₂), 3.96 (t, 2H, *J* = 6.2 Hz, O-CH₂), 6.75–6.79 (m, 4H, Ph-H), 6.92 (d, 2H, *J* = 7.2 Hz, Ph-H), 7.21 (t, 2H, *J* = 8.6 Hz, Ph-H), 9.89 (s, 1H, CONH). ¹³C-NMR (DMSO-*d*₆, 75 MHz): δ 170.20, 154.28, 151.51, 132.17, 129.36, 125.29, 119.20, 116.23, 115.77, 114.50, 113.46, 66.54, 54.95, 53.27, 48.67, 30.84, 26.76, 25.57. HR-MS (ESI) calcd for C₂₂H₂₈N₃O₂⁺ ([M + H]⁺): 366.2176; found: 366.2177.

6-(3-(Morpholino)propoxy)-3,4-dihydroquinolin-2(1H)-one (**2g**) Mp 146–147 °C, yield 79%. ¹H-NMR (DMSO-*d*₆, 300 MHz): δ 1.83–1.92 (m, 2H, CH₂), 2.40–2.46 (m, 8H, CH₂), 2.86 (t, 2H, *J* = 7.3 Hz, N-CH₂), 3.62 (t, 4H, *J* = 4.5 Hz, N-CH₂), 3.94 (t, 2H, *J* = 6.2 Hz, O-CH₂), 6.64–6.79 (m, 3H, Ph-H), 9.85 (s, 1H, N-H). ¹³C-NMR (DMSO-*d*₆, 75 MHz): δ 170.19, 154.26, 132.15, 125.28, 116.22, 114.46, 113.43, 66.67, 66.45, 55.36, 53.85, 30.83, 26.42, 25.56. HR-MS (ESI) calcd for C₁₆H₂₃N₂O₃⁺ ([M + H]⁺): 291.1703; found: 291.1702.

6-(3-(Piperidin-1-yl)propoxy)-3,4-dihydroquinolin-2(1H)-one (**2h**) Mp 138–140 °C, yield 79%. ¹H-NMR (DMSO-*d*₆, 300 MHz): δ 1.78–1.87 (t, 2H, CH₂), 2.38 (t, 2H, *J* = 7.4 Hz, CH₂), 2.47–2.60 (m, 6H, CH₂), 2.60 (s, 4H, CH₂), 2.82 (t, 2H, *J* = 7.4 Hz, CH₂), 3.09 (s, 4H, N-CH₂), 3.24 (s, 2H, N-CH₂), 3.93 (t, 2H, *J* = 6.2 Hz, O-CH₂), 6.69–6.76 (m, 3H, Ph-H), 9.89 (s, 1H, CONH). ¹³C-NMR (DMSO-*d*₆, 75 MHz): δ 170.20, 154.19, 132.18, 125.29, 116.23, 114.51, 113.49, 66.29, 54.48, 49.76, 43.43, 41.15, 30.83, 26.40, 25.56. HR-MS (ESI) calcd for C₁₇H₂₅N₂O₂⁺ ([M + H]⁺): 289.1911; found: 289.1912.

6-(3-(4-Phenylpiperidin-1-yl)propoxy)-3,4-dihydroquinolin-2(1H)-one (**2i**) Mp 174–176 °C, yield 78%. ¹H-NMR (DMSO-*d*₆, 300 MHz): δ 1.27 (s, 1H, CH), 1.79–2.03 (m, 6H, CH₂), 2.30 (s, 2H, *J* = 6.2 Hz, CH₂), 2.49–2.68 (m, 4H, N-CH₂), 2.89 (t, 2H, *J* = 6.2 Hz, N-CH₂), 3.16 (d, 2H, *J* = 7.9 Hz, N-CH₂), 4.00 (s, 2H, *J* = 6.2 Hz, O-CH₂), 6.66–6.81 (m, 3H, Ph-H), 7.18–7.31 (m, 5H, Ph-H), 9.67 (s, 1H, CONH). ¹³C-NMR (DMSO-*d*₆, 75 MHz): δ 170.4, 154.2, 145.7, 131.7, 128.4, 126.7, 126.1, 124.7, 116.1, 114.1, 113.1, 66.2, 55.0, 53.9, 41.8, 32.8, 30.7, 26.3, 25.7. HR-MS (ESI) calcd for C₂₃H₂₉N₂O₂⁺ ([M + H]⁺): 365.2224; found: 365.2223.

6-(2-(Piperidin-1-yl)ethoxy)-3,4-dihydroquinolin-2(1H)-one (**3a**) Mp 147–149 °C, yield 77%. ¹H-NMR (CDCl₃, 300 MHz): δ 1.66–1.97 (m, 8H, CH₂), 2.50 (t, 2H, *J* = 7.3 Hz, CH₂), 2.89 (t, 2H, *J* = 7.3 Hz, CH₂), 3.10 (t, 2H, *J* = 6.0 Hz, CH₂), 3.58 (t, 2H, *J* = 4.7 Hz, CH₂), 4.38 (t, 2H, *J* = 4.7 Hz, O-CH₂), 6.70–6.86 (m, 3H, Ph-H), 9.64 (s, 1H, CONH). ¹³C-NMR (CDCl₃, 75 MHz): δ 175.40, 157.54, 137.55, 129.85, 121.19, 119.28, 118.24, 67.72, 60.80, 58.61, 49.32, 35.43, 30.44, 27.69. HR-MS (ESI) calcd for C₁₆H₂₃N₂O₂⁺ ([M + H]⁺): 275.1754; found: 275.1756.

6-(4-(Piperidin-1-yl)butoxy)-3,4-dihydroquinolin-2(1H)-one (**3b**) Mp 150–151 °C, yield 78%. ¹H-NMR (CDCl₃, 300 MHz): δ 1.58–1.68 (m, 2H, CH₂), 1.82–2.01 (m, 8H, CH₂), 2.62 (t, 2H, *J* = 7.5 Hz, CH₂), 2.75–2.85 (m, 6H, CH₂), 2.96 (t, 2H, *J* = 7.5 Hz, N-CH₂), 3.99 (t, 2H, *J* = 6.1 Hz, O-CH₂), 6.67–6.74 (m, 3H, Ph-H), 7.70 (s, 1H, CONH). ¹³C-NMR (CDCl₃, 75 MHz): δ 170.83, 154.74, 130.82, 125.16, 115.97, 114.69, 113.20, 67.70, 58.00, 53.80, 30.64, 27.00, 25.74, 23.91, 23.06, 21.99. HR-MS (ESI) calcd for C₁₈H₂₇N₂O₂⁺ ([M + H]⁺): 303.2067; found: 303.2068.

6-((5-(Piperidin-1-yl)pentyl)oxy)-3,4-dihydroquinolin-2(1H)-one (**3c**) Mp 150–151 °C, yield 79%. ¹H-NMR (CDCl₃, 300 MHz): δ 1.53–1.63 (m, 4H, CH₂), 1.80–1.89 (q, 4H, CH₂), 2.00–2.11 (m, 6H, CH₂), 2.62 (t, 2H, *J* = 7.4 Hz, CH₂), 2.93–3.01 (m, 6H, -NCH₂), 3.97 (t, 2H, *J* = 6.2 Hz, O-CH₂), 6.66–6.76 (m, 3H, Ph-H), 7.61 (s, 1H, N-H). ¹³C-NMR (CDCl₃, 75 MHz): δ 170.76, 164.81, 130.76, 125.17, 116.93, 114.67, 113.23, 67.66, 57.39, 53.26, 30.66, 28.66, 25.74, 23.67, 23.34, 22.36, 22.02. HR-MS (ESI) calcd for C₁₉H₂₉N₂O₂⁺ ([M + H]⁺): 317.2224; found: 317.2222.

3.1.3. Synthesis Procedure of 1-Alkyl-6-(3-(piperidin-1-yl)propoxy)-3,4-dihydroquinolin-2(1H)-one (**4a-4b**)

Sodium hydroxide (0.12 g, 3 mmol), compound **2h** (0.6 g, 2 mmol), and bromopropane (0.37 g, 3 mmol) were placed into a flask with 20 mL of acetonitrile, and the mixture was refluxed for 24 h. Then the brine was added after evaporating the solvent of the mixture. The combined organic layer was dried over anhydrous MgSO₄ after the extraction with DCM 3 times (30 mL × 3). A crude product was obtained after filtration and evaporation. The residue was purified by silica gel column chromatography with 1% methanol in DCM to obtain the compound **4a**. The bromopropane was replaced by pentane bromide to give the compound **4b**. The characterization for the two compounds is listed below.

6-(3-(Piperidin-1-yl)propoxy)-1-propyl-3,4-dihydroquinolin-2(1H)-one (**4a**) oil, yield 78%. ¹H-NMR (CDCl₃, 300 MHz): δ 0.87 (t, 3H, *J* = 7.5 Hz, CH₃), 1.51–1.63 (m, 4H, CH₂), 1.77–1.85 (m, 4H, CH₂), 2.12–2.21 (m, 2H, CH₂), 2.52 (t, 2H, *J* = 7.4 Hz, CH₂), 2.75–2.85 (m, 8H, CH₂), 3.78 (t, 2H, *J* = 7.5 Hz, N-CH₂), 3.96 (t, 2H, *J* = 6.1 Hz, O-CH₂), 6.65–6.83 (m, 3H, Ph-H). ¹³C-NMR (CDCl₃, 75 MHz): δ 169.63, 154.01, 133.25, 128.12, 115.77, 114.49, 112.61, 65.92, 55.49, 53.91, 43.56, 31.34, 25.76, 25.14, 23.97, 22.97, 20.34, 11.14. HR-MS (ESI) calcd for C₂₀H₃₁N₂O₂⁺ ([M + H]⁺): 331.2380; found: 331.2381.

1-Pentyl-6-(3-(piperidin-1-yl)propoxy)-3,4-dihydroquinolin-2(1H)-one (**4b**) oil, yield 77%. ¹H-NMR (CDCl₃, 300 MHz): δ 0.90 (t, 3H, *J* = 7.1 Hz, CH₃), 1.29–1.72 (m, 10H, CH₂), 2.13 (s, 4H, CH₂), 2.44–2.63 (m, 4H, CH₂), 2.84 (t, 2H, *J* = 6.2 Hz, N-CH₂), 3.18–3.23 (m, 4H, N-CH₂), 3.88 (t, 2H, *J* = 7.5 Hz, N-CH₂), 4.07 (t, 2H, *J* = 4.8 Hz, O-CH₂), 6.70–6.91 (m, 3H, Ph-H). ¹³C-NMR (CDCl₃, 75 MHz): δ 169.61, 153.66, 133.67, 128.31, 115.83, 114.51, 112.58, 65.35, 55.40, 53.57, 42.17, 31.85, 29.03, 26.88, 25.83, 23.99, 22.55, 22.43, 22.07, 14.01. HR-MS (ESI) calcd for C₂₂H₃₅N₂O₂⁺ ([M + H]⁺): 359.2693; found: 359.2694.

3.2. Pharmacological Assays

3.2.1. Luciferase Assay for the H₃R Antagonistic Activity

Luciferase assay was taken to screen the H₃R antagonistic activity of the compounds **2a-2i**, **3a-3c**, and **4a-4b**. PIT was used as the positive control. Firstly, all the target compounds were screened at 5 μM and 50 μM. In addition, the compounds with an inhibitory rate bigger than 50% were subjected to further assay to obtain the IC₅₀. The detailed experimental operations refer to the previous paper [22,31].

3.2.2. In Vivo Pharmacology Tests for the Antiseizure Activity

The antiseizure activity of the compounds **2a-2i**, **3a-3c**, and **4a-4b** was examined through the MES and PTZ models. The neurological safety of the compounds **2h**, **4a**, and **4b** was evaluated by the rotarod test. In the MES test, the definition of protection was the reduction or vanishing of the THLE in mice. In the PTZ test, the seizures were induced through the subcutaneous administration of PTZ (85 mg/kg). The antiseizure activities of the compounds in the PTZ test were evaluated by comparing the convulsion scores in mice between taking the compounds or not. VPA and PIT were used as positive drugs. To explore the anticonvulsive mechanism, compound **4a** (10 mg/kg) was co-injected with RAMH (10 mg/kg). In addition, the THLE was recorded and compared with that of the mice treated by compound **4a** alone. The detailed experimental operations in the MES, PTZ, and rotarod tests refer to our previous paper [22,32]. All the animal experiments were carried out on 4-week-old KunMing male mice weighing from 20 to 25 g. The mice were

housed collectively in polycarbonate cages in groups of 30, where they were maintained on a 12 h light/dark cycle in a temperature controlled (25 ± 2 °C) laboratory with free access to food and water. In the MES and PTZ models, seven animals were used in each group. In the rotarod test, three animals were used in each group. Each animal was used only once. All the experiments referring to animals were applied according to the Guide for the Care and Use of Laboratory Animals and were approved by the Medical Ethics Committee of Jingtangshan University, approval number: 220811002.

3.2.3. Statistics

GraphPad Prism was used to carry out the statistical analysis. In the seizure tests, data were provided as the mean \pm standard error of the mean (SEM). In addition, one-way ANOVA followed by Dunnett's post hoc test was executed for group comparison. The statistical significance was defined when the *p* value < 0.05 [22].

3.2.4. Molecular Docking

The molecular docking was conducted through the Flexible Docking in Discovery Studio 2019 [22]. The 3D structure of H₃R was constructed from the structure-known H₁R protein (PDB ID: 3RZE) by homology modeling [30]. The 3D structures of the compounds **2h**, **4a**, and PIT were constructed by ChemDraw 16.0, energy minimized, and placed into the protein cavity to flexible binding with the homology model of H₃R. After the docking running finished, the binding patterns were provided, and the interactions between the compounds **2h**, **4a**, PIT, and H₃R were analyzed.

4. Conclusions

In this work, a battery of 6-aminoalkoxy-3,4-dihydroquinolin-2(1*H*)-one derivatives were synthesized to screen their H₃R antagonistic activities and evaluate their antiseizure activities. The majority of the target compounds displayed a potent H₃R antagonistic activity. Among them, the compounds **2a**, **2c**, **2h**, and **4a** showed a submicromolar H₃R antagonistic activity. The MES model screened out three compounds (**2h**, **4a**, and **4b**) with antiseizure activity, while all compounds did not show any protective effect for mice against the seizures induced by PTZ. Additionally, the antiseizure mechanism of compound **4a** was proved to be related to H₃R antagonism. The molecular docking of **2h**, **4a**, and PIT with the H₃R protein predicted their possible binding patterns and gave a presentation that **2h**, **4a**, and PIT had a similar binding model with H₃R.

Author Contributions: Conceptualization, Y.H. (Yi Hua) and X.D.; Methodology, M.S.; Software, Y.H. (Yi Hua) and M.S.; Validation, Y.H. (Yushan Huang); Investigation, Y.H. (Yi Hua), Q.G. and Y.L.; Writing—original draft, M.S.; Writing—review & editing, X.D.; Visualization, X.D.; Supervision, X.D. and Y.H. (Yushan Huang); Project administration, X.D.; Funding acquisition, X.D. and Y.H. (Yushan Huang). All authors have read and agreed to the published version of the manuscript.

Funding: The foundation of this research was the National Natural Science Foundation of China (NO.22167017) and the scientific research fund of Jiangxi provincial education department (No. GJJ201004).

Institutional Review Board Statement: The animal study protocol was approved by the Ethics Committee of Jingtangshan University (protocol code 220811002, date of approval: 11 August 2022).

Informed Consent Statement: Not applicable.

Data Availability Statement: Not applicable.

Conflicts of Interest: The authors declare no conflict of interest.

Sample Availability: Samples of the compounds are not available from the authors.

References

1. Panula, P. Histamine receptors, agonists, and antagonists in health and disease. *Handb. Clin. Neurol.* **2021**, *180*, 377–387. [PubMed]
2. Arrang, J.M.; Garbarg, M.; Schwartz, J.C. Auto-inhibition of brain histamine release mediated by a novel class (H3) of histamine receptor. *Nature* **1983**, *302*, 832–837. [CrossRef] [PubMed]
3. Abdulrazzaq, Y.M.; Bastaki, S.M.A.; Adeghate, E. Histamine H3 receptor antagonists-Roles in neurological and endocrine diseases and diabetes mellitus. *Biomed. Pharmacother.* **2022**, *150*, 112947. [CrossRef] [PubMed]
4. Alhusaini, M.; Eissa, N.; Saad, A.K.; Beiram, R.; Sadek, B. Revisiting Preclinical Observations of Several Histamine H3 Receptor Antagonists/Inverse Agonists in Cognitive Impairment, Anxiety, Depression, and Sleep-Wake Cycle Disorder. *Front. Pharmacol.* **2022**, *13*, 861094. [CrossRef]
5. Sadek, B.; Saad, A.; Sadeq, A.; Jalal, F.; Stark, H. Histamine H3 receptor as a potential target for cognitive symptoms in neuropsychiatric diseases. *Behav. Brain. Res.* **2016**, *312*, 415–430. [CrossRef]
6. Zhang, W.; Zhou, M.; Lu, W.; Gong, J.; Gao, F.; Li, Y.; Xu, X.; Lin, Y.; Zhang, X.; Ding, L.; et al. CNTNAP4 deficiency in dopaminergic neurons initiates parkinsonian phenotypes. *Theranostics* **2020**, *10*, 3000–3021. [CrossRef]
7. Lu, C.W.; Lin, T.Y.; Chang, C.Y.; Huang, S.K.; Wang, S.J. Ciproxifan, a histamine H3 receptor antagonist and inverse agonist, presynaptically inhibits glutamate release in rat hippocampus. *Toxicol. Appl. Pharmacol.* **2017**, *319*, 12–21. [CrossRef]
8. Eissa, N.; Azimullah, S.; Jayaprakash, P.; Jayaraj, R.L.; Reiner, D.; Ojha, S.K.; Beiram, R.; Stark, H.; Łażewska, D.; Kieć-Kononowicz, K.; et al. The dual-active histamine H3 receptor antagonist and acetylcholine esterase inhibitor E100 ameliorates stereotyped repetitive behavior and neuroinflammation in sodium valproate-induced autism in mice. *Chem. Biol. Interact.* **2019**, *312*, 108775. [CrossRef]
9. Di Ciano, P.; Hendershot, C.S.; Le Foll, B. Therapeutic Potential of Histamine H3 Receptors in Substance Use Disorders. *Curr. Top Behav. Neurosci.* **2022**, *59*, 169–191.
10. Zhang, L.; Chen, Z.; Ren, K.; Leurs, R.; Chen, J.; Zhang, W.; Ye, B.; Wei, E.; Timmerman, H. Effects of clobenpropit on pentylenetetrazole-kindled seizures in rats. *Eur. J. Pharmacol.* **2003**, *482*, 169–175. [CrossRef]
11. Vohora, D.; Pal, S.N.; Pillai, K.K. Thioperamide, a selective histamine H3 receptor antagonist, protects against PTZ-induced seizures in mice. *Life Sci.* **2000**, *66*, PL297–PL301. [CrossRef] [PubMed]
12. Sadek, B.; Saad, A.; Latacz, G.; Kuder, K.; Olejarz, A.; Karcz, T.; Stark, H.; Kieć-Kononowicz, K. Non-imidazole-based histamine H3 receptor antagonists with anticonvulsant activity in different seizure models in male adult rats. *Drug Des. Devel. Ther.* **2016**, *10*, 3879–3898. [CrossRef] [PubMed]
13. Fu, Q.; Dai, H.; He, P.; Hu, W.; Fan, Y.; Zhang, W.; Chen, Z. The H3 receptor antagonist clobenpropit protects against Abeta42-induced neurotoxicity in differentiated rat PC12 cells. *Pharmazie* **2010**, *65*, 257–260. [PubMed]
14. Dai, H.; Fu, Q.; Shen, Y.; Hu, W.; Zhang, Z.; Timmerman, H.; Leurs, R.; Chen, Z. The histamine H3 receptor antagonist clobenpropit enhances GABA release to protect against NMDA-induced excitotoxicity through the cAMP/protein kinase A pathway in cultured cortical neurons. *Eur. J. Pharmacol.* **2007**, *563*, 117–123. [CrossRef] [PubMed]
15. Mani, V.; Arfeen, M.; Ali, H.M.; Abdel-Moneim, A.H.; Aldubayan, M.; Alhowail, A. Neuroprotective Effect of Clobenpropit against Lipopolysaccharide-Induced Cognitive Deficits via Attenuating Neuroinflammation and Enhancing Mitochondrial Functions in Mice. *Brain Sci.* **2021**, *11*, 1617. [CrossRef]
16. Bhowmik, M.; Khanam, R.; Vohora, D. Histamine H3 receptor antagonists in relation to epilepsy and neurodegeneration: A systemic consideration of recent progress and perspectives. *Br. J. Pharmacol.* **2012**, *167*, 1398–1414. [CrossRef]
17. Sadek, B.; Kuder, K.; Subramanian, D.; Shafiullah, M.; Stark, H.; Łażewska, D.; Adem, A.; Kieć-Kononowicz, K. Anticonvulsive effect of nonimidazole histamine H3 receptor antagonists. *Behav. Pharmacol.* **2014**, *25*, 245–252. [CrossRef]
18. Alachkar, A.; Latacz, G.; Siwek, A.; Lubelska, A.; Honkisz, E.; Gryboś, A.; Łażewska, D.; Handzlik, J.; Stark, H.; Kieć-Kononowicz, K.; et al. Anticonvulsant evaluation of novel non-imidazole histamine H₃R antagonists in different convulsion models in rats. *Pharm. Biochem. Behav.* **2018**, *170*, 14–24. [CrossRef]
19. Dutilleul, P.C.; Ryvlin, P.; Kahane, P.; Vercueil, L.; Semah, F.; Biraben, A.; Schwartz, J.C.; De Seze, J.; Hirsch, E.; Collongues, N. Exploratory Phase II Trial to Evaluate the Safety and the Antiepileptic Effect of Pitolisant (BF2.649) in Refractory Partial Seizures, Given as Adjunctive Treatment During 3 Months. *Clin. Neuropharmacol.* **2016**, *39*, 188–193.
20. Kasteleijn-Nolst Trenité, D.; Parain, D.; Genton, P.; Masnou, P.; Schwartz, J.C.; Hirsch, E. Efficacy of the histamine 3 receptor (H₃R) antagonist pitolisant (formerly known as tiprolisant; BF2.649) in epilepsy: Dose-dependent effects in the human photosensitivity model. *Epilepsy Behav.* **2013**, *28*, 66–70. [CrossRef]
21. Beheshti, S.; Wesal, M.W. Anticonvulsant activity of the histamine H3 receptor inverse agonist pitolisant in an electrical kindling model of epilepsy. *Neurosci. Lett.* **2022**, *782*, 136685. [CrossRef] [PubMed]
22. Xiao, F.; Yan, R.; Zhang, Y.; Wang, S.; Chen, S.; Zhou, N.; Deng, X. Synthesis and antiseizure effect evaluation of nonimidazole histamine H3 receptor antagonists containing the oxazole moiety. *Arch. Pharm.* **2021**, *354*, e2000298. [CrossRef] [PubMed]
23. Wang, S.; Liu, H.; Lei, K.; Li, G.; Li, J.; Wei, Y.; Wang, X.; Liu, R. Synthesis of 3,4-dihydroquinolin-2(1H)-one derivatives with anticonvulsant activity and their binding to the GABAA receptor. *Bioorg. Chem.* **2020**, *103*, 104182. [CrossRef] [PubMed]
24. Wang, S.; Liu, H.; Wang, X.; Lei, K.; Li, G.; Li, J.; Liu, R.; Quan, Z. Synthesis of 1,3,4-oxadiazole derivatives with anticonvulsant activity and their binding to the GABAA receptor. *Eur. J. Med Chem.* **2020**, *206*, 112672. [CrossRef] [PubMed]
25. Deng, X.Q.; Song, M.X.; Zheng, Y.; Quan, Z.S. Design, synthesis and evaluation of the antidepressant and anticonvulsant activities of triazole-containing quinolinones. *Eur. J. Med Chem.* **2014**, *73*, 217–224. [CrossRef] [PubMed]

26. Dressler, H.; Economides, K.; Favara, S.; Wu, N.N.; Pang, Z.; Polites, H.G. The CRE luc bioluminescence transgenic mouse model for detecting ligand activation of GPCRs. *J. Biomol. Screen.* **2014**, *19*, 232–241. [[CrossRef](#)]
27. Shi, Y.; Sheng, R.; Zhong, T.; Xu, Y.; Chen, X.; Yang, D.; Sun, Y.; Yang, F.; Hu, Y.; Zhou, N. Identification and characterization of ZEL-H16 as a novel agonist of the histamine H3 receptor. *PLoS ONE* **2012**, *7*, e42185. [[CrossRef](#)]
28. Reiner, D.; Stark, H. Ligand binding kinetics at histamine H3 receptors by fluorescence-polarization with real-time monitoring. *Eur. J. Pharmacol.* **2019**, *848*, 112–120. [[CrossRef](#)]
29. Sadek, B.; Saad, A.; Schwed, J.S.; Weizel, L.; Walter, M.; Stark, H. Anticonvulsant effects of isomeric nonimidazole histamine H3 receptor antagonists. *Drug Des. Devel. Ther.* **2016**, *10*, 3633–3651. [[CrossRef](#)]
30. Vohora, D.; Pal, S.N.; Pillai, K.K. Histamine as an Anticonvulsant Inhibitory Neurotransmitter. *Curr. Neuropharmacol.* **2004**, *2*, 419–425. [[CrossRef](#)]
31. Shimamura, T.; Shiroishi, M.; Weyand, S.; Tsujimoto, H.; Winter, G.; Katritch, V.; Abagyan, R.; Cherezov, V.; Liu, W.; Han, G.W.; et al. Structure of the human histamine H1 receptor complex with doxepin. *Nature* **2011**, *475*, 65–70. [[CrossRef](#)] [[PubMed](#)]
32. Song, M.; Yan, R.; Zhang, Y.; Guo, D.; Zhou, N.; Deng, X. Design, synthesis, and anticonvulsant effects evaluation of nonimidazole histamine H3 receptor antagonists/inverse agonists containing triazole moiety. *J. Enzym. Inhib. Med Chem.* **2020**, *35*, 1310–1321. [[CrossRef](#)] [[PubMed](#)]

Disclaimer/Publisher’s Note: The statements, opinions and data contained in all publications are solely those of the individual author(s) and contributor(s) and not of MDPI and/or the editor(s). MDPI and/or the editor(s) disclaim responsibility for any injury to people or property resulting from any ideas, methods, instructions or products referred to in the content.